

Analyst

Accepted Manuscript



This is an *Accepted Manuscript*, which has been through the Royal Society of Chemistry peer review process and has been accepted for publication.

Accepted Manuscripts are published online shortly after acceptance, before technical editing, formatting and proof reading. Using this free service, authors can make their results available to the community, in citable form, before we publish the edited article. We will replace this *Accepted Manuscript* with the edited and formatted *Advance Article* as soon as it is available.

You can find more information about *Accepted Manuscripts* in the [Information for Authors](#).

Please note that technical editing may introduce minor changes to the text and/or graphics, which may alter content. The journal's standard [Terms & Conditions](#) and the [Ethical guidelines](#) still apply. In no event shall the Royal Society of Chemistry be held responsible for any errors or omissions in this *Accepted Manuscript* or any consequences arising from the use of any information it contains.

Cite this: DOI: 10.1039/x0xx00000x

Raman spectroscopic studies of vitamin A content in the liver: a biomarker of healthy liver

Received 00th January 2012,
Accepted 00th January 2012

DOI: 10.1039/x0xx00000x

K. Kochan,^{1,2} K.M. Marzec¹, E. Maslak¹, S. Chlopicki^{1,3} and M. Baranska^{1,2,*}

www.rsc.org/

Confocal Raman microspectroscopy was used in this study to identify hepatic stellate cells (HSCs) from healthy mice and mice with untreated and treated liver steatosis. We have identified the main form of occurrence of vitamin A in healthy liver and confirmed its absence in pathological state. Additionally, we reported the reappearance of vitamin A in tissue after treatment of liver steatosis.

Liver, due to the variety and diversity of its functions, is one of the key organs for the proper functioning of a body. It is involved in many processes, including metabolism, storage of glycogen and vitamins, synthesis of proteins and hormones, decomposition of red blood cells as well as detoxification.¹ Due to the multiplicity and complexity of liver functions, the pathogenesis of many liver diseases is not fully understood. However, in comparison to other organs, liver has a huge potential to regenerate itself. For this reason, many of the liver diseases do not give any clear symptoms until an advanced stage of its damage.

One of the major liver functions, closely associated with the development of pathological changes, is storing vitamins, mainly vitamin A. Vitamin A is a general term, which refers to a group of compounds, among which the most important are retinol, retinal and retinoic acid². In the case of vitamin A, liver plays a key role not only in its storage, but also in its metabolism and control of distribution in the body, *f.e.* through synthesis of retinol-binding protein (RBP)³. Two types of liver cells: hepatocytes (parenchymal cells) and hepatic stellate cells (HSCs) are involved in processing and storing vitamin A⁴. Hepatocytes are mainly involved in the processes related to the uptake and transformation of vitamin A as well as its distribution, through the synthesis (and secretion) of RBP. These cells account for approximately 70% of the liver cells and contain about 90% of total liver proteins^{5,6}. HSCs, on the

other hand, are the primary storage of vitamin A, holding approximately 50–60% of retinoids present in healthy organism. They cover only around 8% of liver cells and 1% of the total amount of proteins present in liver^{5,6}. Moreover, liver not only controls the storage and metabolism of retinoids but is also a very important target for many retinoid actions³. Retinoid acid – synthesized in liver – can interact with retinoids receptors in liver, regulating *i.a.* the expression of genes involved in fat metabolism^{7,8}. For this reason, there is a close relationship between the content of retinoids in the liver and the appearance and development of diseases. Disturbances in retinoid signaling, as a consequence of disorders of vitamin A metabolism, are in fact related to hepatic diseases. It concerns particularly HSCs, as upon any liver injury they undergo cellular activation. The activation process embraces transformation from a quiescent to myofibroblastic phenotype^{3,5}. One of the early events, occurring during activation, is a decrease of vitamin A content in HSCs^{9,10}. An association between distorted metabolism of vitamin A and different liver diseases, including cirrhosis, fibrosis, carcinoma, non-alcoholic and alcoholic fatty liver has been reported. The progressive loss of vitamin A storage with the development of the disease has also been demonstrated¹¹.

Raman spectroscopy (RS) was proved multiple times to be an excellent tool allowing for a very detail insight into the studied sample¹²⁻²⁰. Due to its multiple advantages, such as non-destructivity, lack of complicated sample preparation and the possibility to obtain chemical and spatial information about all of the sample components at one time makes it a very attractive technique for the study of biological materials. Furthermore, due to the fact that it provides information on a molecular level, this technique has a big potential in terms of investigating the pathogenesis of diseases by following their progression as well as possibly in the future for early diagnosis.

1 An additional application of RS in the context of biological
2 samples is to evaluate the effectiveness of therapy. This
3 requires however to determine the changes occurring with the
4 disease development as well as define some markers, indicating
5 improvement.

6 Here we present the results of Raman
7 microspectroscopic imaging of vitamin A within liver tissue
8 under different conditions: healthy, diseased and treated. We
9 have previously reported the presence of vitamin A in healthy
10 (normal) liver tissue²⁰. In this work we attempt to characterise it
11 in a more accurate way, confirm its absence (or presence) in
12 disease and more importantly – investigate results of the
13 effective treatment on the vitamin A storage in liver. In order to
14 verify the results two separate models of disease were used.

15 Experimental

16 Livers were obtained from wild-type male C57BL/6J mice. The
17 control group consisted of mice fed with a control diet (AIN-93G,
18 a standard diet for early grow and reproduction). The first
19 pathological model induced by 10 weeks of feeding mice with High
20 Fat (HF) diet, containing 60% of kcal from saturated fat, represents
21 mild hepatic changes, mainly associated with simple steatosis.
22 Subsequently, mice from this group were divided into two, and the
23 metformin treatment was added for the next 5 weeks for one of
24 them. The second model was based on a combination of HF and
25 methionine-choline deficient (MCD) diet (8 weeks of feeding) and
26 represents more severe hepatic alteration (steatosis, inflammation,
27 mild fibrosis). In this case, metformin treatment was introduced after
28 4 weeks of feeding and maintained for the next 4 weeks. This
29 approach allowed to investigate strictly the impact of medical
30 treatment. Each group contained 6 individuals. From each individual
31 at least 2 sections were exanimate and from every section
32 approximately 5 maps were measured. The mice included in the
33 experiment, at the time of its start were 6 weeks old. Differences in
34 the length of feeding regime between two presented models are
35 a result of varying length of time needed to develop the disease,
36 as a result of nutrition.

37 The mice were euthanized by injection of ketamine with
38 xylazine. The whole livers were collected. Immediately after
39 collection livers were frozen in Optimal Cutting Temperature (OCT)
40 medium in -80°C. Samples were subsequently cut into sections of 10
41 µm thickness in a cryostat chamber (Leica CM 1950) in -23°C.
42 Sections were placed on CaF₂ slides, fixed with 4% buffered
43 formalin solution for 10 minutes and rinsed in distilled water (2×5
44 min) in order to remove residues of fixative.

45 Raman measurements were performed with a WITec Confocal
46 Raman Microscope (WITec alpha300 R, Ulm, Germany) equipped
47 with 600 grooves/mm grating, an air cooled solid state laser
48 operating at 532 nm and a CCD detector, cooled to -60°C. Maps
49 were collected using a dry Olympus MPLAN (100×/0.90NA)
50 objective. Spectra were recorded in the range 0 – 3705 cm⁻¹, with the

spectral resolution of 3 cm⁻¹ and integration time 0.3 – 0.5 s. The
laser power was approximately 10 mW. Raman measurements were
controlled using Witec Control software. The size of measured areas
differ, as they were chosen manually. They did not however exceed
the size of 20 µm × 20 µm (per map). The spectra were collected
every 0.36 µm. Approximately, every map contained ~ 3000 spectra
(depending on the exact size of mapped area).

Data analysis was performed in Witec Project Plus
software. Preprocessing included cosmic spike removal (CRR) and
background subtraction with polynomial fit (order 2). Maps of
distribution based on integration of chosen marker bands were obtain
prior to preprocessing. *K – means* cluster (KMC) analysis was
performed on the preprocessed data, with the use of Manhattan
distance and Ward's algorithm. Number of classes was usually 3.

Results and discussion

Vitamin A in healthy liver

Our previous study showed the presence of vitamin A in
healthy liver [20]. In this study vitamin A was also identified in
the healthy (control) group (Fig. 1).

The distribution of organic matter (based on the integration
of C–H stretching region in the range 2800–3050 cm⁻¹) showed
the areas of higher intensity of signal. Those areas correspond
directly to lipids, due to their strong dispersion, what can be
confirmed by the distribution of lipids based on the integration
of a band at 1444 cm⁻¹ (CH₂ scissoring). The lipid-rich
structures may correspond for example to lipid droplets. The
other possibility is hepatic stellate cells, which in case of
control would be expected to be filled with vitamin A.

The prosthetic group of heme of haemoglobin (Hb) provides
strong resonance enhancement when the excitation wavelength
is in resonance with the intense electronic transitions centered
at around 525 nm (Q_v or α band)²¹⁻²⁴. The use of the 532 nm
excitation laser line allows also for observations of the pre-
resonance Raman spectrum of retinols²⁵. Resonance effect
observed for Hb and vitamin A increases the sensitivity and
selectivity of detection of both groups of compounds in
comparison with other tissue components for which non-
resonant Raman spectra are observed. This is due to selective
enhancement of specific chromophores of both compounds and
increase intensity of resonance Raman scattering bands. This
allowed us to detect and analyse vitamin A content even at low
concentrations. Vitamin A shows a very intense marker band
located at approximately 1595 cm⁻¹, as well as other, less
intense bands, *i.a.* located at 1203 and 1165 cm⁻¹. The
distribution map of vitamin A based on the integration of the
band at 1595 cm⁻¹ clearly indicated that some (but not all) of
the lipid-rich structures visible within this map are in fact
HSCs, rich in vitamin A.

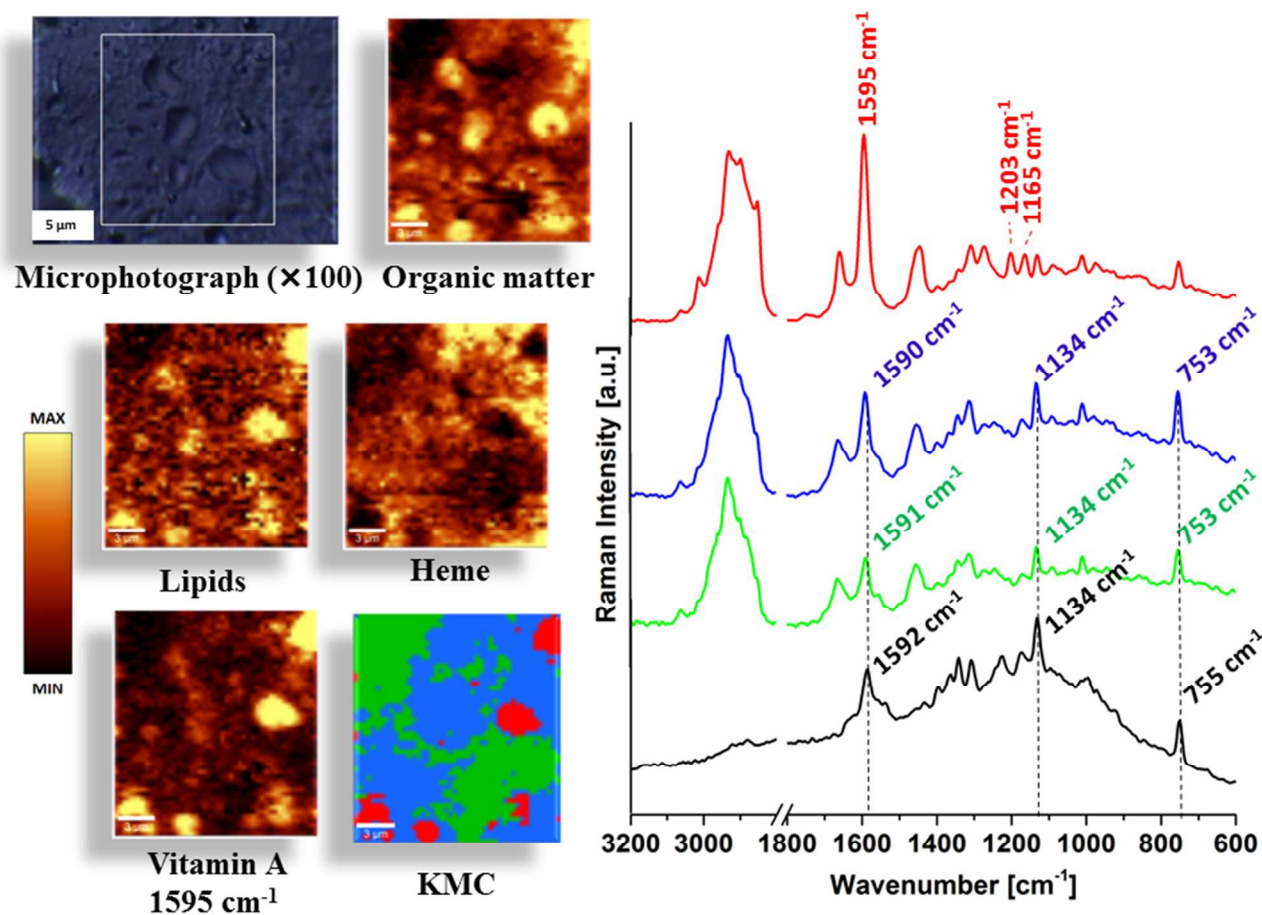


Fig. 1. A microphotograph ($\times 100$) of control liver tissue section with measured area marked by a white square along with the results of: distribution analysis based on the integration of bands in ranges: $2800 - 3050 \text{ cm}^{-1}$ (*organic matter*), $1420 - 1460 \text{ cm}^{-1}$ (*lipids*), $740 - 775 \text{ cm}^{-1}$ (*heme*), $1590 - 1600 \text{ cm}^{-1}$ (*vitamin A*) along with the results of *k - means* cluster analysis (KMC), in the range $600 - 1800 \text{ cm}^{-1}$: distribution of classes and corresponding spectra with marked bands from vitamin A (*in red*) and heme (*in green/blue/black*) along with spectrum of haemoglobin standard (*in black*). Size of mapped area: $16.6 \mu\text{m} \times 18.4 \mu\text{m}$ (46×51 points).

It is important to underline here, that in the case of liver tissue the vitamin A marker band (1595 cm^{-1}) is located closely to one of the marker bands of heme ($\sim 1590 \text{ cm}^{-1}$). Since liver tissue is rich in heme, a band located at around $1590 - 1600 \text{ cm}^{-1}$ will be present in the entire map; however it may originate from vitamin A or heme. Heme can be recognized, apart from this band, by an increasing background in the region $600 - 1800 \text{ cm}^{-1}$ (due to resonant effect) or the presence of two other characteristic bands: at 755 and 1135 cm^{-1} . However, the increasing of the background may also result from the use of high laser power. Haemoglobin can absorb a considerable amount of photons due to the presence of the closely packed heme group, what can result in an additional effect of raised background. The use of relatively high laser power (for biological material) creates a possibility of such effect. Moreover, as the degree of packing of heme groups can vary within the mapped area of the tissue, the raise of the background due to the thermal effect described above could also vary, even while the use of the same laser power. In order

to confirm that the band at 1595 cm^{-1} originates from vitamin A (not heme) and in fact the integration of this band shows HSCs location, a map of distribution based on different heme marker band (755 cm^{-1}) is presented. As can be seen, the areas corresponding to the highest intensity of the band at 1595 cm^{-1} are at the same time characterised by the lowest intensity of heme bands. Besides of that they also have intense lipid signal, which additionally confirms that they are HSCs.

KMC results remain in compliance with the results of analysis based on integration of marker bands. The red class – corresponding to HSCs – showed a greater intensity of signals from lipids, as well as the presence of vitamin A signals. At the same time the bands originating from heme are clearly lower in intensity. Additionally, the red class showed the presence of other vitamin A marker bands, absent in other classes. The blue and green class differed mainly in the concentration of heme (different intensities of the bands at 753 , 1134 and 1590 cm^{-1} and different degree of increase background due to the presence of heme).

For a more detailed insight into the HSCs composition spectra were compared with the measured spectra of standards of retinol, retinal and retinoic acid (Fig.2.). Band positions along with their assignment are listed in Table 1. As can be seen, the main (most intense) marker band for retinal (1572 cm^{-1}

¹) and retinoic acid (1576 cm^{-1}) is clearly shifted towards lower wavenumber, as compared to retinol (1594 cm^{-1}). A comparison between spectra of standards and the average spectrum from HSCs indicated clearly that their main component is retinol.

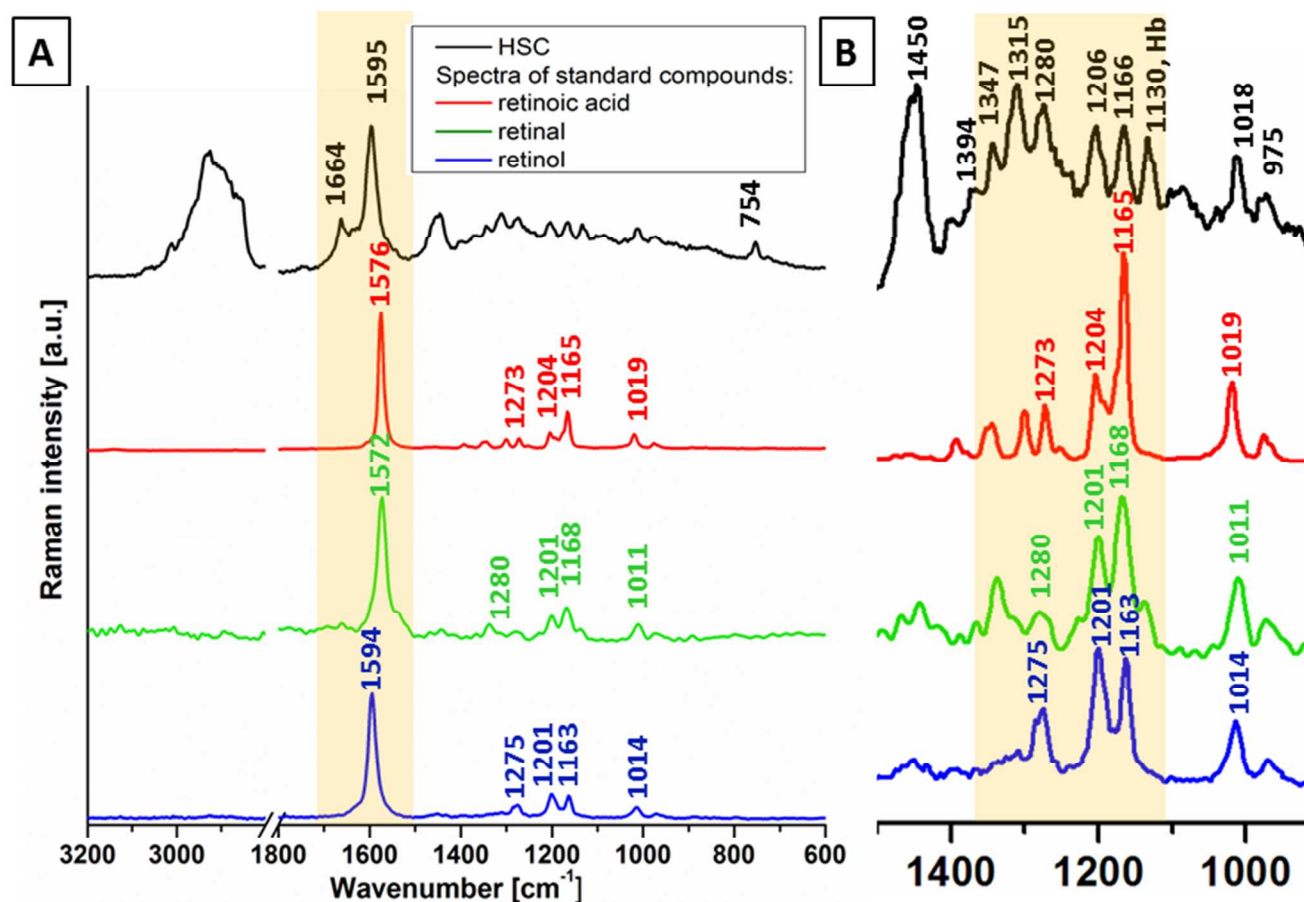


Fig.2. The average spectrum obtained from 10 different hepatic stellate cells (HSCs) extracted from liver tissue from high concentration of vitamin A compared with Raman spectra of standard compounds of all-*trans* retinol, all-*trans* retinal and all-*trans* retinoic acid in (A) the range $3200 - 600\text{ cm}^{-1}$ and (B) enlarged range $1500 - 950\text{ cm}^{-1}$.

Table 1. Band positions along with their assignment for retinol, retinal and retinoic acid standards.

Band position [cm^{-1}]			Assignment
Retinol	Retinal	Retinoic acid	
1594	1572	1576	$\nu(\text{C}=\text{C})$
1275	1280	1273	$\rho(\text{CCH})$
1201	1201	1204	$\nu(\text{C}-\text{C})$
1163	1168	1165	$\nu(\text{C}-\text{C})$
1014	1011	1019	$\rho(\text{C}-\text{CH})_3$

Disease influence on vitamin A storage

Liver studies showed that in case of any abnormalities, related to the various lifestyle diseases (diabetes, cardiovascular diseases) vitamin A was not detected. In case of liver from mice

model C57BL/6J on both mixed: High Fat (HF) diet and Methionine-Choline-Deficient (MCD) diet as well as just HF (standard dietary model of Non-Alcoholic Fatty Liver Disease, NAFLD) the vitamin A was not observed in any of the measured maps. This is in accordance with the current state of knowledge, stating that vitamin A is used up during the first stage of the development of pathological changes in liver^{9,10}.

Treatment impact: regeneration of vitamin A storage

Loss of vitamin A in the liver tissue due to development of the disease indicates the possibility of using it as a marker of liver damage. However, liver is known to have a big potential for regeneration. The withdrawal of pathological changes can be caused by successful medical treatment. In order to investigate the changes that occur as a result of treatment with respect to vitamin A, mice with developed NAFLD were subjected to treatment with metformin, used as a reference drug. The effectiveness of therapy was evident, among others, due to

a clear reduction of liver steatosis. Under such conditions, an attempt was made to investigate the HSCs in terms of the presence of vitamin A. Examples of an analysis, corresponding to the one for control tissue, for samples from HF and HF +

MCD diet after metformin treatment are presented on figures 3 and 4.

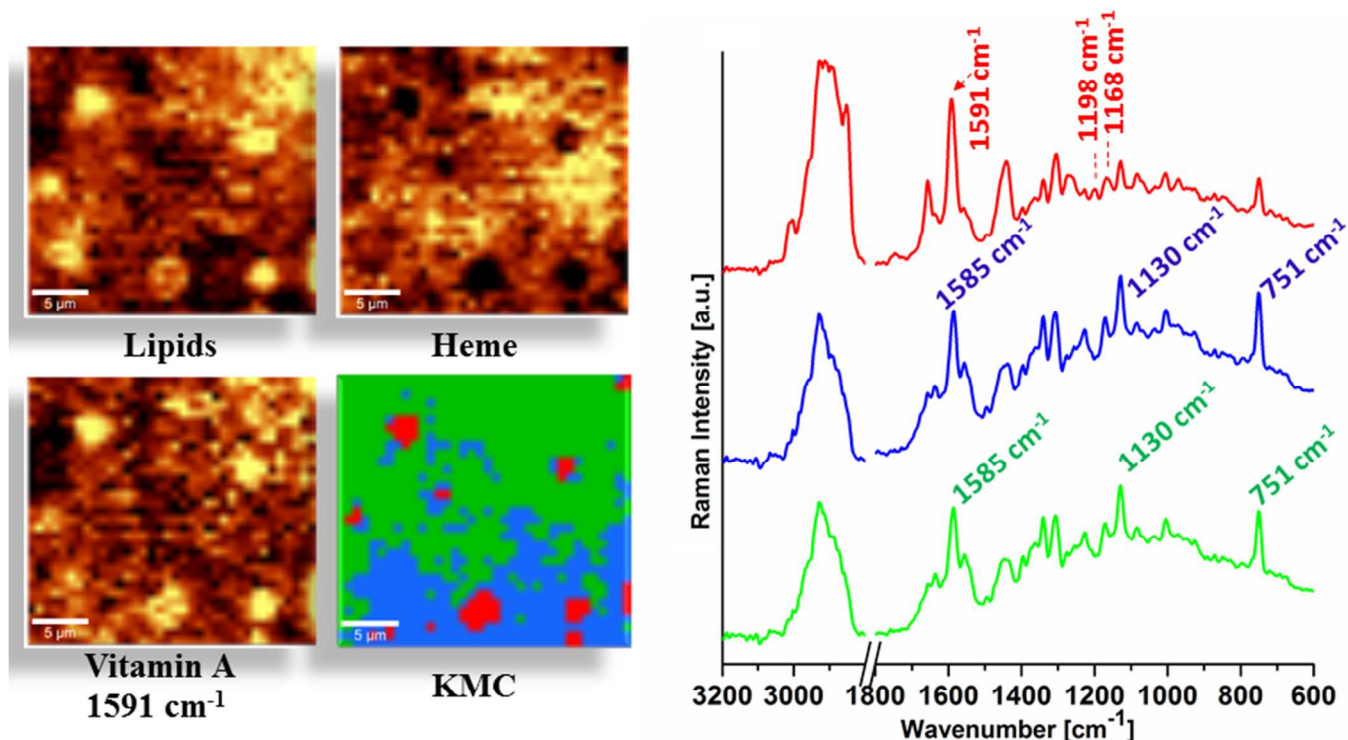


Fig. 3. Results for a liver tissue section with NAFLD induced by HF diet and treated with metformin. The distribution analysis based on the integration of bands in ranges: $1420 - 1460 \text{ cm}^{-1}$ (lipids), $740 - 775 \text{ cm}^{-1}$ (heme) and $1590 - 1600 \text{ cm}^{-1}$ (vitamin A) along with the results of *k*-means cluster analysis (KMC), in the range $600 - 1800 \text{ cm}^{-1}$: distribution of classes and corresponding spectra with marked bands from vitamin A (in red) and heme (in green/blue). Size of mapped area: $25.9 \mu\text{m} \times 24.1 \mu\text{m}$ (72×70 points).

Interestingly, the presence of vitamin A in HSCs can be detected in both models of disease after treatment. As can be seen, again the distribution of lipids indicated the presence of lipid-rich structures. In this case the analysis required special carefulness, as there was a considerable probability (significantly higher than for the control sections) that those structures are lipid droplets, manifesting the most characteristic pathological disorder of fatty liver. However, the distribution of vitamin A, based on the integration of the band at $1591 (1592) \text{ cm}^{-1}$ indicated its presence within some of those structures. At the same time, the areas of high intensity of this band correspond to the areas with a low content of heme (based on the integration of the band at 755 cm^{-1}). KMC results confirmed this conclusion, by separating a red class with more intense lipid signals and at the same time clearly lower heme signals (751 cm^{-1} , 1130 cm^{-1}). The intensity of the band at $1591 (1592) \text{ cm}^{-1}$ was raised, in comparison to green and blue class. This change was, however, not followed by a change of intensity of other heme bands (which were less intense in the red class), what allowed to conclude that in this case the band at $1591 (1592) \text{ cm}^{-1}$ can also be assigned to vitamin A.

In the liver samples after treatment the signal from vitamin A was weaker as compared to control samples (compare the ratio of $1595/1444$ and $1591/1444 \text{ cm}^{-1}$ for both red classes in Fig.1 and 3). Furthermore, the bands at 1164 cm^{-1} and 1198 cm^{-1} , clearly visible in spectra from HSCs in control samples (1165 and 1203 cm^{-1}) were poorly visible in the ones from treated samples. This may be due to a lower content of vitamin A in HSCs after treatment. In fact, HSC lose vitamin A while there are activated by *f.e.* proinflammatory state and during regression of pathology the storage of vitamin A is not as rapid. Stellate cells from control samples were filled with vitamin A as they serve as a storage of it. However, it is being used during the first stage of development of fatty liver. Under effective treatment, in addition to various changes, including *f.e.* a reduction of lipid droplets size, the vitamin A is being restored in HSCs again. However, due to the fact that the storage of vitamin A is being rebuilt, the intensity of its signals is lower. It should also be emphasized at this point that the decreased intensity of the signals of vitamin A can also result from an increase of the fraction of lipids, which would cause an impression of lower content of vitamin A.

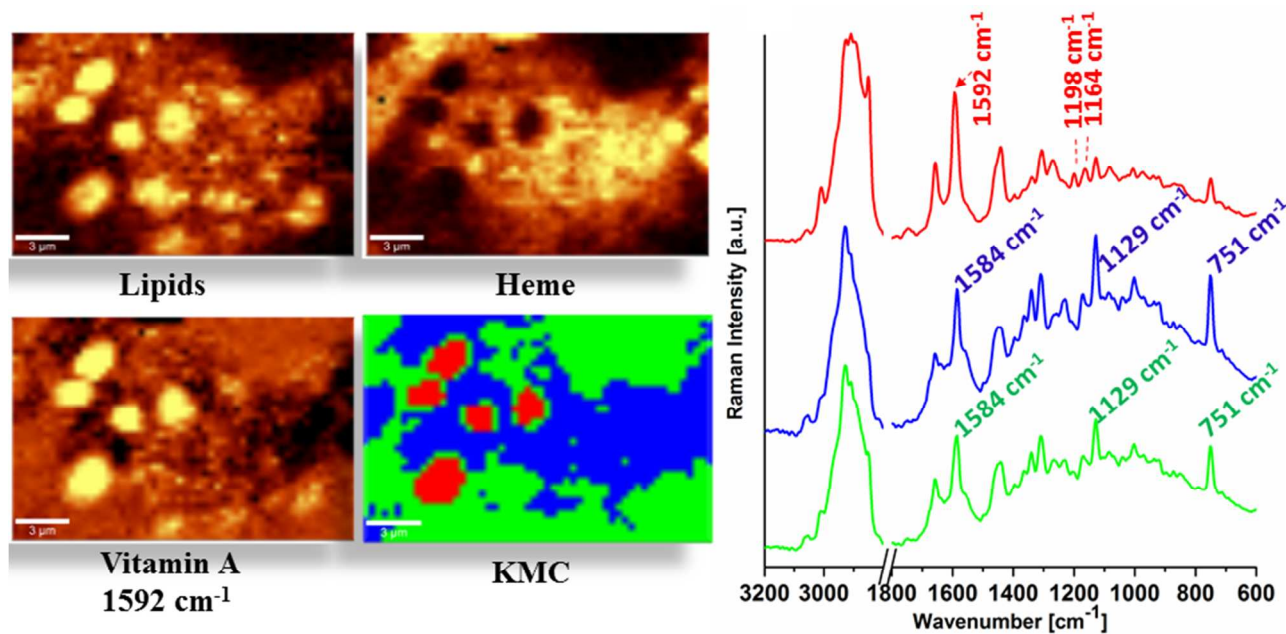


Fig. 4. Results of: distribution analysis based on the integration of bands in ranges: $1420 - 1460 \text{ cm}^{-1}$ (*lipids*), $740 - 775 \text{ cm}^{-1}$ (*heme*) and $1590 - 1600 \text{ cm}^{-1}$ (*vitamin A*) along with the results of *k-means* cluster analysis (KMC), in the range $600 - 1800 \text{ cm}^{-1}$: distribution of classes and corresponding spectra with marked bands from vitamin A (*in red*) and heme (*in green/blue*) for a liver tissue section with NAFLD induced by HFD+ MCD and treated with metformin. Size of mapped area: $19.3 \mu\text{m} \times 12.6 \mu\text{m}$ (54×35 points).

Conclusions

We presented the possibility of Confocal Raman microspectroscopy for detection of single specific cells (HSCs) within the liver tissue. It allowed us to identify the presence of vitamin A and to provide information about the main form of its occurrence as retinol. We confirmed the lack of vitamin A due to the development of the disease on the example of non-alcoholic fatty liver. Above all, we report the reappearance of vitamin A in HSCs in liver tissue after successful treatment, wherein the effectiveness of therapy was confirmed as it manifested itself in different ways. This result was observed in two different models of disease. Therefore, we suggest that the storage of vitamin A is rebuilt even after injury, under favorable conditions, to which undoubtedly belongs successful therapy. Thus, we conclude that the liver content of vitamin A may serve as a marker of liver health status.

Notes and references

¹Jagiellonian Centre for Experimental Therapeutics (JCET), Jagiellonian University, Krakow, Poland,

²Faculty of Chemistry, Jagiellonian University, Krakow, Poland.

³Department of Experimental Pharmacology, Jagiellonian University, Krakow, Poland

*email: baranska@chemia.uj.edu.pl

Acknowledgements

This work was supported by the European Union under the European Regional Development Fund (grant coordinated by JCET-UJ, POIG.01.01.02-00-069/09) and National Science Center (grant DEC-2013/09/N/NZ7/00626 and UMO-2012/07/D/ST4/02214). KK acknowledges the Marian Smoluchowski Krakow Research Consortium: "Matter Energy Future" (granted the KNOW status for the 2012-2017 by the Ministry of Science and Higher Education) scholarship.

- 1 M. Al-Mahtab, S. Rahman, *Liver: A Complete Book on Hepato-Pancreato-Biliary Diseases*, Reed Elsevier India Private Limited, 2009.
- 2 O. Fennema, *Fennema's Food Chemistry*, CRC Press Taylor & Francis, ISBN: 9780849392726, p.454 - 455.
- 3 Y. Shirakami *et al.*, *BiochimBiophys Acta*, 2012, **1821**(1), 124 - 136.
- 4 W. S. Blaneret *et al.*, *BiochimBiophys Acta*, 2009, **1791**, 467 - 473.
- 5 S.L.Friedman *et al.*, *Physiol Rev.*, 2008, **88**, 125 - 172.
- 6 A. Geertset *et al.*, *Semin Liver Dis.*, 2001, **31**, 311 - 335.
- 7 J.E. Balmeret *et al.*, *J Lipid Res.*, 2002, **43**, 1773 - 1808.
- 8 M.M. McGraneet *et al.*, *J Nutr Biochim*, 2007, **18**, 497 - 508.
- 9 R. Batalleret *et al.*, *J Clin Invest*, 2005, 115, 209 - 218.
- 10 S. L. Friedman *et al.*, *J Biol Chem*, 2000, **275**, 2247 - 2250.
- 11 M. A. Leo *et al.*, *N Engl J Med*, 1982, **307**, 597 - 601.

Journal Name

- 12 M. Diem *et al.*, *J. Biophotonics*, 2013, **6**(11–12), 855– 886.
- 13 C. Krafft, *et al.*, *Proc. SPIE 8207, Photonic Therapeutics and Diagnostics VIII*, 2012, 820741 .
- 14 B. R. Woodet *et al.*, *J. Biomed. Opt.*, 2005, **10**(1), 14005.
- 15 F. Bonnier *et al.*, *Vibrational Spectroscopy*, 2012, **61**, 124-132.
- 16 S. Sivakumar *et al.*, *Spectrochim Acta A Mol Biomol Spectrosc.*, 2014, **118**, 461–469.
- 17 C. Krafft *et al.*, *Vib. Spectrosc.*, 2011, **55**, 90 – 100.
- 18 S. Zhang *et al.*, *J.Chem. Phar. Res.*, 2013, **5**(11), 45– 48.
- 19 K. Majzner *et al.*, *Anal Chem*, 2014, **86**(13), 6666 – 6674.
- 20 K. Kochan *et al.*, *Analyst*, 2013, **38**, 3885 – 3890.
- 21 Streaks T.C. *et al.*, *J Raman Spec*, 1973, **1**, 197 – 206.
- 22 Yamamoto T., *et al.*, *J Biol Chem*, **1973**, 248, 5211 – 5213.
- 23 Kitagawa T., *The heme protein structure and the iron histidine stretching mode*, in: T.G Spiro (Ed.), *Biological Applications of Raman Spectroscopy, Resonance Raman Spectra of Heme and Metalloproteins*, Wiley, New York, 1988,, Vol. 3, pp. 97–131.
- 24 Nagatomo S., *et al.*, *J Am Chem Soc*, 2011, **133**, 10101 – 10110.
- 25 Galler K. *et al*, *Integr Biol*. 2014, **6**, 946 – 956.